EUROPEAN JOURNAL OF CANCER 47 (2011) 305–315

available at www.sciencedirect.com

ScienceDirect

journal homepage: www.ejconline.com

Organ specific regulation of tumour invasiveness and gelatinolytic activity at the invasive front ☆

Elin Hadler-Olsen [a,*], *Hilde Ljones Wetting* [b], *Chandra Ravuri* [a], *Ahmad Omair* [a], *Oddveig Rikardsen* [c], *Gunbjørg Svineng* [a], *Premasany Kanapathippillai* [a], *Jan-Olof Winberg* [a], *Lars Uhlin-Hansen* [a,d]

[a] *Department of Medical Biology, Faculty of Health Sciences, University of Tromsø, Norway*
[b] *Department of Pharmacy, Faculty of Health Sciences, University of Tromsø, Norway*
[c] *Ear Nose and Throat Department, University Hospital of North Norway, Tromsø, Norway*
[d] *Department of Pathology, University Hospital of North Norway, Tromsø, Norway*

ARTICLE INFO

Article history:
Received 25 June 2010
Received in revised form 19 August 2010
Accepted 2 September 2010

Keywords:
Oral cancer
Skin cancer
Animal model
Tumour invasiveness
Matrix metalloproteinases
Gelatinolytic activity

ABSTRACT

Proteolytic enzymes play a complex role in tumour growth and invasion. To explore the impact of tumour stroma on invasiveness and expression of proteolytic enzymes, we used a xenograft mouse model where tumours in tongue and skin were established from various human cancer cell lines. Gelatinolytic activity in the tumours was investigated by a novel *in situ* zymography technique which enables high image resolution. *In vivo* and *in vitro* expression of various proteolytic enzymes were analysed at transcriptional and protein level using RT-qPCR, immunohistochemistry and SDS–PAGE substrate zymography. At the mRNA level all cell lines were found to express MMP-2, -7, -14, uPA and uPAR. In addition, two out of three cell lines expressed MMP-9. Histological analyses revealed that tongue tumours had an invasive growth pattern, associated with reduced E-cadherin expression. In contrast, the skin tumours established from the same cell lines were non-invasive. Tongue tumours of all cell lines showed strong gelatinolytic activity especially at the invasive front, which was not seen in the non-invasive skin tumours. Our results show a close relationship between tumour invasiveness and gelatinolytic activity at the tumour front. Furthermore, in our model, both invasiveness and activity of tumour-associated proteolytic enzymes were more dependent on the tumour microenvironment than on inherent properties of the cancer cells.

1. Introduction

Oral squamous cell carcinomas (SCCs) are characterised by an aggressive behaviour with frequent lymph node metastases and a poor survival rate.[1] In contrast, skin SCCs seldom metastasize and are usually curable.[2] This marked difference in progression of SCCs arising in two different environments may be due to inherent properties of the cancer cells or local factors in the oral cavity and the skin. Stromal cells may regulate cancer progression by release of cytokines, growth

☆ The Norwegian Cancer Society, The Erna and Olav Aakre Foundation for Cancer Research and The North Norwegian Health Authorities.

* *Corresponding author:* Address: Department of Medical Biology, Faculty of Health Sciences, University of Tromsø, 9037 Tromsø, Norway. Tel.: +47 77645846; fax: +47 77644680.
E-mail address: elin.hadler-olsen@uit.no (E. Hadler-Olsen).

0959-8049/$ - see front matter © 2010 Elsevier Ltd. All rights reserved.
doi:10.1016/j.ejca.2010.09.006

factors, proteases and extracellular matrix (ECM) molecules which modulate growth and invasion of cancer cells.[3,4]

Proteases, in particular matrix metalloproteases (MMPs) have complex roles in cancer development and progression.[5,6] They can promote cancer cell migration by cleaving ECM proteins and affect tissue homeostasis by processing various non-ECM proteins such as chemokines, growth factors, cytokines, cell receptors and intercellular adhesion molecules.[7–9] Processing of the epithelial adhesion molecule E-cadherin can trigger epithelial-to-mesenchymal transition (EMT) which increases the invasiveness of cancer cells.[10] Paracrine interactions in the tumour–stroma interface have been shown to induce MMP-expression in both cancer cells and stromal cells.[11,12] Also the composition of the ECM can affect MMP expression and activity, as demonstrated with collagen I and MMP-2.[13] High expression levels of various MMPs in tumour cells and/or the stromal compartment are correlated with cancer progression and poor prognosis in many cancer types.[14] Most of these former studies have focused on the expression of MMPs by immunohistochemistry and RT-PCR, and not on enzyme activity. In contrast, *in situ* zymography is an appropriate method for detection and localisation of enzymatic activity. This method has so far been performed on frozen tissue sections.[15,16] Due to the poor morphology of the frozen sections, detailed localisation of the enzymatic activity has been difficult to determine. We have recently refined the *in situ* zymography method by applying this technique on tissue fixed in a zinc based fixative (ZBF).[16] Compared to standard *in situ* zymography on frozen sections, our new *in situ* zymography technique enables high image resolution.

We have established a xenograft model of oral and skin cancer to investigate the impact of the tumour microenvironment on growth and progression of carcinomas. In the present work we studied the growth pattern of various cancer cells in the two environments and investigated if invasive growth is reflected in the expression and activity of proteolytic enzymes. Using *in situ* zymography, we demonstrate that the tumours growing in the tongue have much more gelatinolytic activity compared to the corresponding tumours growing in the skin, especially at the invasive front. Our results show that the tumour microenvironment has a profound impact on cancer cell associated gelatinolytic activity, as well as on invasive growth.

2. Materials and methods

2.1. Cell culture

Cell lines and culture media are listed in Table 1. The skin SCC cell line UT-SCC-12A was a kind gift from Professor R. Grénman, University of Turku, Finland, established as described in Grénman and colleagues, 1992,[17] and the oral SCC cell line HSC-4 was generously provided by Professor M. Yanagishita, Tokyo Medical and Dental University, Japan. The endometrial adenocarcinoma cell line Ishikawa was purchased from Sigma Aldrich (St. Louis, MO), and the NHDF cell line was from Lonza Walkersville, Inc (Walkersville, MD). All cell lines were incubated in a humidified atmosphere of 5% CO_2 at 37 °C.

2.2. Animals and establishment of xenograft tumours

BALB/c nude mice (Harlan Laboratories, Indianapolis, IN) were anaesthetised with Ketamine and Xylazine hydrochloride before suspensions of the different cell lines (300,000 cells/25 μl 0.9% NaCl) were injected into the anterior of the tongue or subcutaneously on the abdomen. To ensure that the mice did not suffer more than 10% weight loss, they were weighed every second day and were sacrificed after 15–28 d of tumour growth. Tumours were either fixed in ZBF or submerged in RNA later (Sigma–Aldrich). Blood samples were collected and plasma isolated. The project was approved by the Norwegian Animal Research Authority and conducted in accordance with FELASA guidelines.

2.3. Immunohistochemistry

Immunohistochemistry was performed on sections of ZBF-fixed, paraffin-embedded tongue and skin tumours with the primary antibodies listed in Table 2. Horseradish peroxidase (HRP)-labelled secondary antibody and di-aminobenzidine substrate were used for visualisation (EnVision$^+$ system-HRP,

Table 1 – Cell lines and culture media.

Cell line	Origin	Medium
HSC-4	Lymph node metastasis of tongue SCC	Dulbecco's modified eagle medium (DMEM), 10% FBS, 0.5 mM L-glutamine, 50 U/ml penicillin and 50 μg/ml streptomycin
UT-SCC-12A	Skin SCC, nose	DMEM, 10% FBS, 0.5 mM L-glutamine, 50 U penicillin and 50 μg/ml streptomycin, 0.1 mM non-essential amino acids
Ishikawa	Endometrial adenocarcinoma	Royal Park Memorial Institute (RPMI) 1640 medium, 10% FBS, 0.5 mM L-glutamine, 50U Penicillin and 50 μg/ml streptomycin
NHDF	Normal human dermal fibroblasts (adult skin)	DMEM, 10% FBS, 0.5 mM L-glutamine, 50 U penicillin and 50 μg/ml streptomycin, 0.1 mM non-essential amino acids

The same medium without FBS was used for the respective cell lines for generation of conditioned medium for SDS–PAGE substrate zymography and Western blotting.

Table 2 – Antibodies used in immunohistochemistry.

Antibody	Dilution	Incubation
Rabbit anti-human E-cadherin, #3195 from Cell Signaling Technology, Danvers MA	1:300	Over night, 4 °C
Rabbit anti-human MMP-2, # ab37150, Abcam Cambridge, MA	1:350	30 min., room temperature (RT)
Rabbit anti-human MMP-9, # ab38898, Abcam Cambridge, MA	1:1000	30 min., RT

Dako, Glostrup, Denmark). Staining was performed as previously described.[16] Sections in which the primary antibody was replaced by 1.5% (v/v) normal goat serum were used as negative controls.

Immunohistochemical staining of the tumour cells was scored according to Kobel and colleagues.[18] Proportion of tumour cells with positive staining (membrane staining for E-cadherin) was scored as no cells stained (0), <10%, (1), 10–50% (2), 51–80% (3) or >80% (4). In addition the intensity of the staining was scored as weak (1), moderate (2) or strong (3). The final score was determined by multiplication of these two variables. For MMP-2 and MMP-9, stromal staining was also scored as negative (0), weak/few positive cells (1), moderate/positive cells surrounding more than half of the tumour (2) or strong/positive cell surrounding the whole tumour (3). Staining intensity was assessed in the whole tumour and in the surrounding stroma in a 0.5 mm radius from the tumour. For each cell line and implantation site 3 individual tumours were analysed.

2.4. *In situ zymography*

Gelatinolytic activity was localised by *in situ* zymography on ZBF-fixed tumour samples of tongue and skin tumours of the various cell lines as described earlier.[16] To verify the contribution of metalloproteases, 20 mM EDTA was added to the substrate in control sections. The level of auto-fluorescence in the tissue was evaluated by incubating control sections at −20 °C. Fluorescence was studied using a Leica TSC SP5 confocal laser microscope with Leica Application Suite Advanced Fluorescence software (Leica, Wetzlar, Germany). Gelatinolytic activity was assessed in the whole tumour and in the surrounding stroma in a 0.5 mm radius from the tumour. For each cell line and implantation site 4 individual tumours were analysed.

2.5. *RNA extraction*

Tumour samples stored in RNAlater (Sigma–Aldrich) were prepared under a dissecting microscope to separate tumour from stroma and further homogenised in a TissueLyzer (Qiagen, Hilden, Germany). Total RNA was extracted using RNeasy Fibrous Tissue Mini kit (Qiagen) according to the manufacturer's instructions. RNA was also extracted from the cell lines grown *in vitro* using RNeasy Mini kit from Qiagen. On-column DNase treatment of the RNA samples was performed using RNase-Free DNase (Qiagen) according to the product manual. The quantity and purity of the extracted RNA were determined using a NanoDrop spectrophotometer (Thermo Fisher Scientific, Wilmington, DE). RNA integrity was assessed using an Experion automated electrophoresis system (Bio-Rad Laboratories, Hercules, CA).

2.6. *Reverse transcription quantitative PCR (RT-qPCR)*

The mRNA expression levels in cell lines and tissue samples were quantified by reverse transcription quantitative PCR (RT-qPCR) (Stratagene Mx3000P instrument, Stratagene, La Jolla, CA). The MMP-primers were designed using Primer Express v.2.0 (Applied Biosystems, Foster City, CA) and synthesised by Eurogentec (Eurogentec, SA, Searing, Belgium), and primers for uPAR, uPA and reference genes were from Qiagen (Tables 3 and 4). A final concentration of 300 nM of each primer was used. Reverse transcription of total RNA was performed using QuantiTect Reverse Transcription Kit (Qiagen) with 300 ng of RNA per 20 μl cDNA reaction. cDNA corresponding to 5,4 ng RNA was amplified for 40 cycles in a 25 μl PCR mix (RT^{2}Real-Time™ SYBR Green/ROX PCR Master Mix (SA Biosciences, Frederick, MD)). Cycling conditions: 95 °C for 10 min, 40 cycles at 95 °C for 30 s, 55 °C for 1 min and 72 °C for 30 s. Primer specificities and absence of primer

Table 3 – Sequences of primers synthesised by Eurogentec.

Gene symbol	Forward primer (5′–3′) Reverse primer (5′–3′)	Amplicon length (bp)	RefSeq accession number
hMMP2	TGGGACAAGAACCAGATCACATA CGAGCAAAGGCATCATCCA	83	NM_004530.4 NM_001127891.1
hMMP9	CCACCACAACATCACCTATTGG GAAGGCGCGGGCAAA	85	NM_004994.2?
hMMP7	GGATGGTAGCAGTCTAGGGATTAACT GGAATGTCCCATACCCAAAGAA	79	NM_002423.3
hMMP14	GCCTGCGTCCATCAACACT ACACCCAATGCTTGTCTCCTTT	77	NM_004995

Abbreviations: *h*; human, *MMP;* matrix metalloproteinase.

Table 4 – Primer sets purchased from Qiagen.

Gene symbol	AssayName	Cat.No	Amplicon length (bp)	RefSeq accession number
hPLAUR	Hs_PLAUR_1_SG	QT00076447	109	NM_001005376 NM_001005377 NM_002659
hPLAU	Hs_PLAU_1_SG	QT00013426	116	NM_001145031 NM_002658
hTFRC	Hs_TFRC_1_SG	GT00095431	146	NM_001101
hACTB	Hs_ACTB_1_SG	QT00095431	146	NM_001101

Abbreviations: *h*, human; *PLAUR*, plasminogen activator, urokinase receptor; *PLAU*, *plasminogen* activator, urokinase; *TFRC*, transferrin receptor; *ACTB*, β-actin.

dimmers were determined by SYBR green melting curve analysis. Duplicate reverse transcriptase reactions were performed for each RNA sample, and duplicate PCR analyses were performed on each cDNA sample. Absence of genomic DNA was confirmed by a no reverse transcription control, and absence of contaminations was assessed by including a no template control in every run. The ΔΔCt method[19] was used to determine the relative amount of target gene in the samples, normalising against the average expression of the two reference genes *TFRC* and *ACT-B*.

2.7. *In vitro secretion of MMPs and plasminogen activators*

To analyse secreted enzymes, 40,000 and 80,000 cells were seeded per cm^2 in the serum containing media listed in Table 1. After 16 h, cells were rinsed 3 times with serum-free medium before 125 μl per cm^2 serum-free medium was added. Conditioned medium was harvested after 48 h incubation, and loose cells were removed by centrifugation (6000 rpm for 5 min at 4 °C). HEPES (pH 7.5) and $CaCl_2$ were added to a final concentration of 0.1 M and 10 mM, respectively. In addition, Ishikawa cells were cultured in conditioned serum-free media harvested from the NHDF cell line. Medium was harvested after 72 h, and treated as described above. Experiments were done in triplicate.

2.8. *Gelatin zymography*

Undiluted or 32× diluted cell-conditioned media, and 20× diluted plasma were analysed by SDS–PAGE substrate zymography as described previously.[16] Gels contained 0.1% (w/v) gelatin in both the separating and stacking gel. The stacking gel contained 4%, and the separating gel 7.5% or 10% (w/v) polyacrylamide. Parallel gels were run with 0.1% (w/v) plasminogen in addition to gelatin to assess presence of plasminogen activators in the samples. To evaluate the enzyme classes responsible for the observed gelatinolytic activity, three parallel gels were run. One was washed and incubated in buffers containing 10 mM EDTA (a metalloprotease inhibitor), the second in buffers containing 1 mM Pefabloc (a serine protease inhibitor) and the third gel in buffers without inhibitors (control).

2.9. *Statistics*

Two tailed *t*-tests were used to evaluate differences between tongue and skin tumours for the different parameters analysed. Data are presented as means ± standard error of the mean (SEM). Independent replicates (N) for the different data are identified in tables and figure legends. *P*-values < 0.05 were accepted as statistically significant. Statistical analyses were performed using SPSS 15.0 for Windows.

3. Results

3.1. *Morphological features*

Tumours of human cancer cell lines were established in the tongue or the skin of mice.

Cancer cells at the invasive front of the tongue tumours showed an invasive growth with single cells or small groups of cells infiltrating the surrounding stroma (Fig. 1A, C and E). In contrast, skin tumours were clearly separated from the

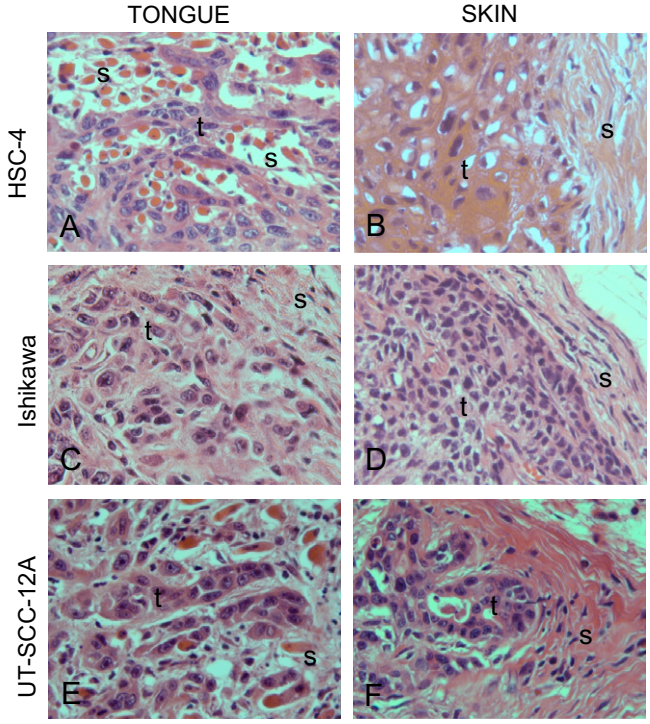

Fig. 1 – Invasive front of tongue and skin tumours. H/E staining of tongue (A, C, E) and skin (B, D, F) tumours of the oral SCC cell line HSC-4 (A, B), the endometrial adenocarcinoma cell line Ishikawa (C, D) and the skin SCC cell line UT-SCC-12A (E, F). Original magnification: 400x. Labelling indicates: t, tumour; s, stroma.

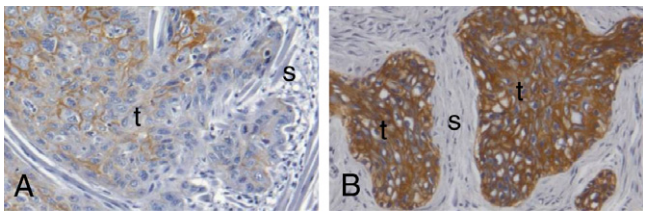

Fig. 2 – Immunohistochemical E-cadherin staining of tongue and skin tumours. Immunohistochemical E-cadherin staining of tumours of the oral SCC cell line HSC-4 in tongue (A) and skin (B). E-cadherin staining is shown in brown, cell nuclei are stained blue. Labelling indicates: t, tumour; s, stroma. Original magnification: 100×. The pictures are representative of three independent experiments.

stromal tissue, often with a prominent fibrous, capsule like tissue (Fig. 1B, D and F). Also, cancer cells at the invasive front of the tongue tumours had more irregular nuclei and contained more cytoplasm than the corresponding skin tumours. Tongue tumours of the HSC-4 cell line showed a marked decrease in E-cadherin staining towards the invasive front (Fig. 2A), whereas the HSC-4 skin tumours had a uniform and much stronger E-cadherin staining (Fig. 2B) (score: tongue 7.3 ± 0.7 vs. skin 12.0 ± 0, $P = 0.02$). Ishikawa and UT-SCC-12A tumours showed weak and fragmented E-cadherin expression both in tongue and skin, compared to the HSC-4 cell line (data not shown).

3.2. *Gelatinolytic activity*

Assessed by *in situ* zymography, the tongue tumours of all cell lines showed stronger gelatinolytic activity than the corresponding skin tumours (Fig. 3A, C, E versus B, D and F). In the tongue tumours the gelatinolytic activity increased towards the invasive front of the tumour, and were especially prominent in cancer cells that were invading the surrounding stroma (Fig. 3A, C and E), whereas the non-invasive skin tumours showed uniform, weak activity (Fig. 3B, D and F). Gelatinolytic activity was also increased in stroma close to the tumours compared to what was seen at a distance from the tumours in both tongue and skin. The tumour stroma in the skin often showed stronger activity than the cancer cells (Fig. 3B and F). Gelatinolytic activity in tumours as well as in stroma was almost completely inhibited by EDTA (Fig. 3G and I), indicating that metalloproteases were responsible for most of the observed activity. Incubation at −20 °C inhibited all activity, showing that the level of auto-fluorescence in the tissues was very low (Fig. 3H and J).

At the cellular level, single cells at the invasive front of tongue tumours showed gelatinolytic activity concentrated in spots (Fig. 4A–C). In some cells the activity was most pronounced towards the cell membrane and at the cell surface (Fig. 4A and B), whereas others showed strong perinuclear activity (Fig. 4C).

3.3. *Expression of proteolytic enzymes*

Tongue and skin tumours of all cell lines were immunohistochemically stained for the major gelatin-degrading enzymes MMP-2 and MMP-9. MMP-2 staining was mainly confined to the tumour cells (Fig. 5A and B). Tumours of the HSC-4 cell line showed stronger MMP-2 staining in tongue than in skin (score: 8 ± 0 versus 4 ± 0, $P = 0.001$), whereas tongue and skin tumours of the UT-SCC-12A (Fig. 5A and B) and Ishikawa cell lines showed similar staining. Cancer cells in tongue and skin tumours of all cell lines were negative for MMP-9, whilst strong staining was seen in subgroups of stromal cells closely surrounding the tumour islands (Fig. 5C and D). The number of MMP-9 positive cells surrounding the tumours was higher in the tongue than in the skin for all cell lines (score: 1.5 ± 0.3 versus 0.3 ± 0.2, $P = 0.009$). Based on their morphology, most of these cells were neutrophils.

Analysis of total RNA extracted from the cancer cells grown *in vitro* and from the tongue tumours showed that all cell lines expressed *MMP2, MMP7, MMP14, uPA* (*plau*) and *uPAR* (*plaur*). In addition, HSC-4 and UT-SCC-12A cells also expressed *MMP9* mRNA. Expression of most enzymes was upregulated *in vivo* compared with *in vitro* (Table 5).

SDS–PAGE substrate zymography was performed on serum-free conditioned medium from the different cell lines to study their secretion of gelatinolytic enzymes and plasminogen activators (PAs). The gelatin zymography gels showed a band at around 60 kDa and weaker bands at 72 and 92 kDa for the HSC-4 cell line, whilst no bands were seen for the Ishikawa cell line (Fig. 6A, upper panel). The UT-SCC-12A cell line showed a strong band at 72 kDa and only faint bands at 92, 60 and 45 kDa. EDTA inhibited all observed activity, whilst Pefabloc had no effect on the intensity of any band, demonstrating that the secreted enzymes were metalloproteases (data not shown). The bands at 92, 72 and 60 kDa probably represent proMMP-9, proMMP-2 and active MMP-2 respectively. The band seen at 45 kDa in UT-SCC-12A cells may represent one of the collagenases, MMP-1 or MMP-13.

All cell lines expressed the pro-MMP2 activator MMP-14 (Table 5), and experiments were performed to verify that the MMP-14 produced by these cell lines was active. Ishikawa cells, which do not secrete MMP-2 (Fig. 6A, upper panel), were incubated in serum-free conditioned medium from the fibroblast cell line NHDF, which secretes large amounts of proMMP-2, but no active forms. On gelatin zymography gels, this combined conditioned medium gave a new band of approximately 62 kDa, consistent with active MMP-2. (Fig. 6B, lane 3). As controls, the serum-free conditioned medium from NHDF cells was incubated in empty wells, and Ishikawa cells were incubated in serum-free medium. The control NHDF-conditioned medium showed only the proMMP-2 band of 72 kDa on zymography gels, confirming that the 62 kDa active band was not due to autoactivation (Fig. 6B, lane 2), whereas the Ishikawa-conditioned medium showed no gelatinolytic bands (Fig. 6B, lane 4). This strongly indicates that Ishikawa cells produce active MMP-14, capable of processing proMMP-2 to an active form.

Addition of plasminogen to the gels (Fig. 6A, lower panel) revealed additional bands to those seen in the gelatin zymography gels (Fig. 6A, upper panel), and these are PAs. Strong PA bands from all cell lines were detected at approximately 55 kDa, probably representing high Mr uPA. This band was particularly strong in the HSC-4 cells, which also produced a PA with a Mr around 37 kDa, probably representing a low Mr uPA.

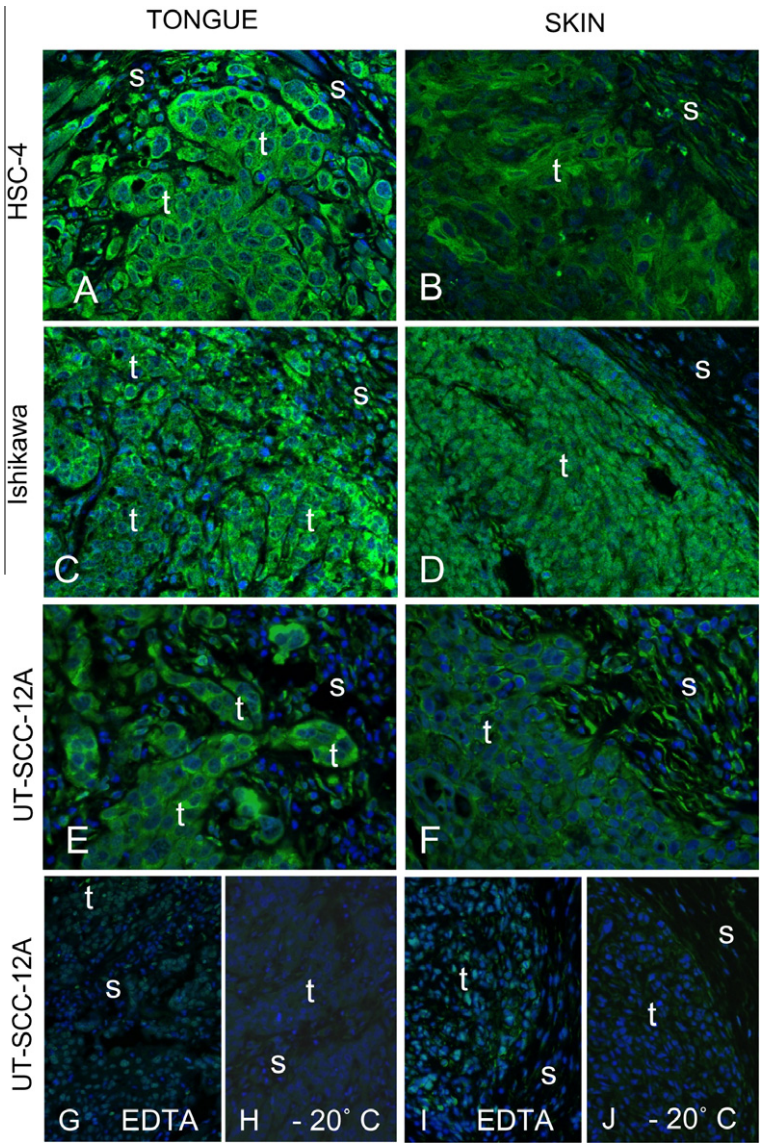

Fig. 3 – *In situ* zymography of tongue and skin tumours. *In situ* zymography with DQ-gelatin as substrate of tumours of the oral SCC cell line HSC-4 in tongue (A) and skin (B), the endometrial adenocarcinoma cell line Ishikawa in tongue (C) and skin (D) and the skin SCC cell line UT-SCC-12A cell line in tongue (E, G and H)) and skin (F, I and J). Green fluorescence (FITC) represents gelatinolytic activity, whilst cell nuclei are blue (DAPI). To demonstrate the contribution from metalloproteases, 20 mM of EDTA was added to substrate (G, I). As a control of auto-fluorescence in the tissue, sections were incubated at –20 °C (H and J). Labelling indicates: t, tumour; s, stroma. These pictures are representative of four independent experiments. Original magnifications: 630× (A and B), 400× (C–F) or 200× (G–J).

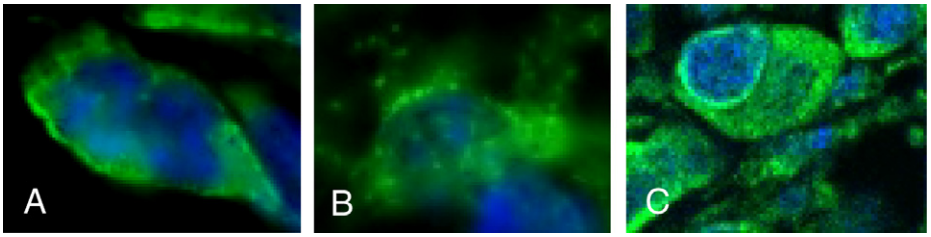

Fig. 4 – *In situ* zymography of tongue tumours. Pictures show *in situ* zymography of single cells at the invasive front of tongue tumours using DQ-gelatin as substrate. Green fluorescence (FITC) shows gelatinolytic activity, whilst cell nuclei are blue (DAPI). (A) and (B) UT-SCC-12A; (C) HSC-4.

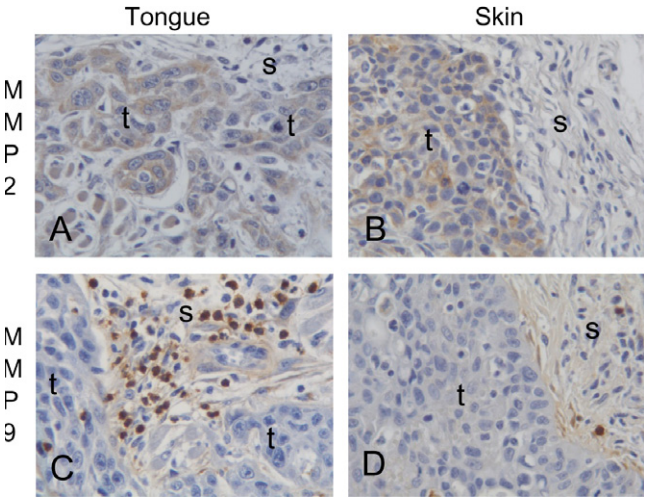

Fig. 5 – Immunohistochemical MMP-2 and MMP-9 staining of tongue and skin tumours. Immunohistochemical MMP-2 staining of tumours of the skin SCC cell line UT-SCC-12A in (A) tongue and (B) skin. Immunohistochemical MMP-9 staining of tumours of the skin SCC cell line UT-SCC-12A in tongue (C) and skin (D). MMP-2/-9 staining is shown in brown, cell nuclei are stained blue. Labelling indicates: t, tumour; s, stroma. Original magnification: 400×. These pictures are representative of three independent experiments.

3.4. *Gelatinolytic enzymes in plasma*

To investigate if the invasive tongue tumours expressed more circulating gelatinolytic enzymes than the non-invasive skin tumours, plasma from the tumour-bearing mice was analysed by SDS–PAGE gelatin zymography. Plasma from mice with tongue tumours of the HSC-4 cell line contained gelatinolytic enzymes with molecular weights of approximately 235, 215, 145 and 110 kDa that were either absent, or present in very small amounts in plasma from mice with skin tumours of the same cell line (Fig. 7, lower panel). For the other cell lines, no consistent differences were seen between mice with tongue and skin tumours (Fig. 7, upper panel). Pefabloc inhibited enzymes with Mr of approximately 25, 80 and 140 kDa, demonstrating that these bands represented serine proteases, whilst all other enzymes were inhibited by EDTA, consistent with being metalloproteases (Fig. 7, lower panel). Addition of plasminogen to the gel revealed that plasminogen activators were present in the plasma, although there were no differences between the various tumour-bearing mice (data not shown).

4. Discussion

To study to what extent the different aggressiveness of oral and skin SCCs may be due to intrinsic properties of the cancer cells or the microenvironment in the two locations, we have studied heterotopic and orthotopic growth of human SCC cell lines from the oral cavity and the skin in a xenograft mouse model. In addition, an endometrial adenocarcinoma cell line which is heterotopic in both skin and tongue was used. In the present study we found that the tongue tumours had a more infiltrative growth pattern and stronger gelatinolytic activity than the skin tumours established from the same cell lines. Our results clearly indicate that the tumour microenvi-

Table 5 – mRNA expression levels in vitro and *in vivo* quantified by RT-qPCR.

Gene	Cell line	ΔCt[a]		Mean fold change[b] in gene expression (*in vivo*/*in vitro*)± SEM
		In vitro	*In vivo*	
MMP2	HSC-4	13.0	6.6	87.9 ± 12.3
	Ishikawa	13.6	6.9	102.9 ± 21.0
	UT-SCC-12A	8.2	4.2	16.2 ± 1.1
MMP7	HSC-4	13.3	12.5	1.8 ± 0.1
	Ishikawa	15.6	10.0	46.0 ± 8.5
	UT-SCC-12A	1.0	0.3	1.7 ± 0.05
MMP9	HSC-4	18.6	15.6	7.7 ± 1.7
	Ishikawa	ND	ND	ND
	UT-SCC-12A	18.9	14.5	20.7 ± 4.2
MMP14	HSC-4	3.8	2.2	3.1 ± 0.2
	Ishikawa	5.9	4.3	3.1 ± 0.1
	UT-SCC-12A	4.4	2.7	3.1 ± 0.2
uPA	HSC-4	1.6	1.1	1.5 ± 0.1
	Ishikawa	8.4	6.7	3.3 ± 0.1
	UT-SCC-12A	2.1	0.8	2.4 ± 0.3
uPAR	HSC-4	6.2	7.6	0.4 ± 0.04
	Ishikawa	9.4	9.3	1.1 ± 0.8
	UT-SCC-12A	6.0	5.3	1.6 ± 0.2

Abbreviations: Ct, threshold cycle; MMP, matrix metalloproteinase; uPA, urokinase plasminogen activator; uPAR, urokinase plasminogen activator receptor; ND, expression not detectable.

[a] $\Delta Ct = (Ct_{target} - Ct_{reference})$. A smaller ΔCt value indicates a higher mRNA expression level.

[b] Fold change = $2^{-\Delta\Delta Ct}$, where $\Delta\Delta Ct = (Ct_{target} - Ct_{reference})_{in\ vivo} - (Ct_{target} - Ct_{reference})_{in\ vitro}$ $N = 1$ for *in vitro*, $N = 3$ for *in vivo*.

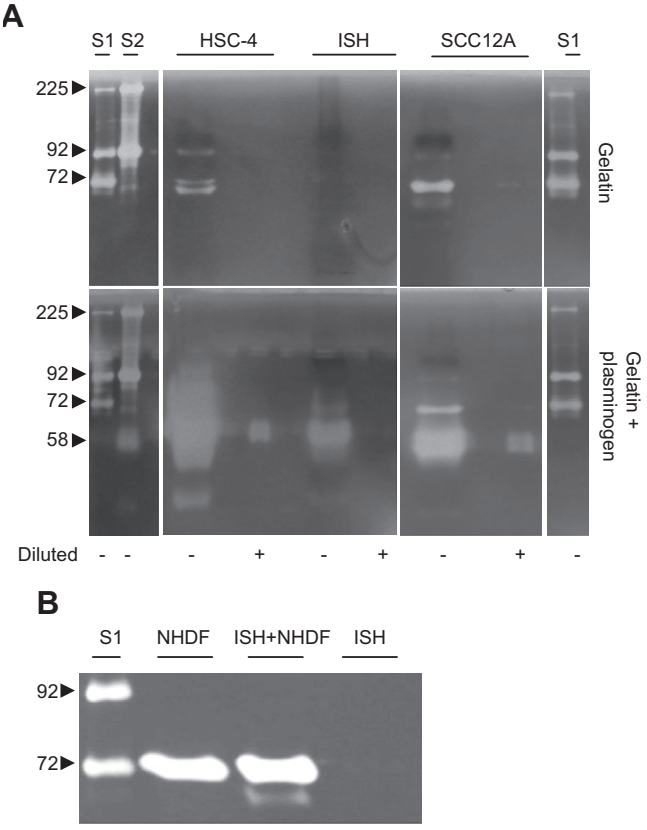

Fig. 6 – Substrate zymographies of serum-free conditioned medium. (A) SDS–PAGE substrate zymography of serum-free conditioned medium of the oral SCC cell line HSC-4, the endometrial adenocarcinoma cell line Ishikawa and the skin SCC cell line UT-SCC-12A grown *in vitro*. Samples are either undiluted (diluted-) or diluted 1:32 (diluted+). The molecular weight standard S1 contains pro-MMP-9 dimer (225 kDa), pro-MMP-9 monomer (92 kDa) and pro-MMP-2 (72 kDa), whilst the molecular weight standard S2 contains pro-MMP-9 dimer (225 kDa), pro-MMP-9 monomer (92 kDa) and plasminogen activator (58 kDa). Upper panel: gelatin gel. Lower panel: gelatin gel with co-polymerised plasminogen. Representative gels from at least three independent experiments are shown. (B) SDS–PAGE gelatin zymography of serum-free conditioned medium of the normal dermal fibroblast cell line NHDF, the endometrial adenocarcinoma cell line Ishikawa incubated 72 h with serum-free conditioned media of the NHDF cell line (ISH + NHDF) and the Ishikawa cell line (ISH) alone. The molecular weight standard S1 contains pro-MMP-9 monomer (92 kDa) and pro-MMP-2 (72 kDa). Representative gels from three independent experiments are shown.

ronment in tongue, but not in skin, induces an invasive cancer cell phenotype.

Increased expression of MMPs at the invasive front of tumours has been reported earlier.[20] However, most of these former studies have analysed expression of proteolytic enzymes by RT-PCR or immunohistochemistry. Due to the complex post-translational regulation of protease activity, such techniques cannot reliably predict actual enzyme activity.[21,22] By the use of *in situ* zymography, we demonstrated increased proteolytic activity towards the invasive front of the tongue tumours, particularly pronounced in tumour cells with an EMT-like appearance. Voessler and colleagues reported that gelatinolytic activity was initiated at the onset of invasive growth, mainly in the tumour stroma.[23] In addition to increased stromal activity, we also found strong gelatinolytic activity at the surface of and within the cancer cells. Pericellular proteolytic activity is known to facilitate cell migration. Association with cell surface proteins may protect the proteases from soluble inhibitors by steric hindrance and promote precise direction of enzymatic activity in infiltrating cells.[20] We found that the intracellular gelatinolytic activity of the tumour cells at the invasive front was most prominent in the periphery of the cells, and was focally distributed, suggesting that active proteolytic enzymes were located within vesicles. Intracellular vesicles containing pro-and active MMP-2 and/or MMP-9 are described within both cancer cells and endothelial cells. In melanoma cells such vesicles have been demonstrated to be actively propelled along microtubules towards the plasma membrane.[24] Trypsin-2 a MMP-9 activator is found co-localised with MMP-9 in intracellular vesicles in oral SCC cells,[25] whilst the MMP-2 activators TIMP-2 and MT1-MMP have been found in association with intracellular gelatinase-containing vesicles in endothelial cells.[26] Such vesicles may facilitate prompt responses to requirements of pericellular proteolytic activity. Many proteins are known to cycle between the cell surface and the cytoplasm of cells, such as uPAR/uPA/PAI1 complexes and MMP-14.[27,28] An increase in pericellular proteolytic activity at the invasive front may lead to increased cycling of proteolytic enzymes with a subsequent increase in intracellular proteolytic activity.

Almost all activity observed by *in situ* zymography was inhibited by EDTA, indicating that metalloproteases were the main contributors to this activity. All cell lines expressed MMP-2, its activator MMP-14 and the MMP-9 activator MMP-7. In addition, HSC-4 and UT-SCC-12A cells also expressed *MMP9* mRNA, although we could not detect MMP-9 protein in the tumour cells *in vivo* by immunohistochemistry. This may be due to different sensitivities of the methods, or alternatively the RNA might not be translated. Proteases cooperate in intricate networks and activation cascades, the so-called protease web. The activity of one enzyme in this network can therefore modulate the net proteolytic potential of a whole system.[29] Proteases produced by stromal cells, such as MMP-9 in the present study, may therefore induce gelatinolytic activity in the cancer cells in the tumour–stroma interface by activating latent pro-enzymes or by releasing growth factors that stimulate protease production. Such paracrine tumour–stroma interactions have been demonstrated in colon cancer as well as in ovarian cancer.[11,12] Functional cooperation between MMPs and members of the plasminogen activator system is thought to exist during physiological and pathological remodelling processes.[30,31] uPA can process plasminogen to the MMP-activator and gelatinolytic enzyme plasmin. We found that all tumour cell lines produced high levels of plasminogen activators as well as the urokinase plasminogen receptor uPAR. uPAR tends to cluster in focal adhesions and cell–cell contacts upon uPA binding. This mechanism is

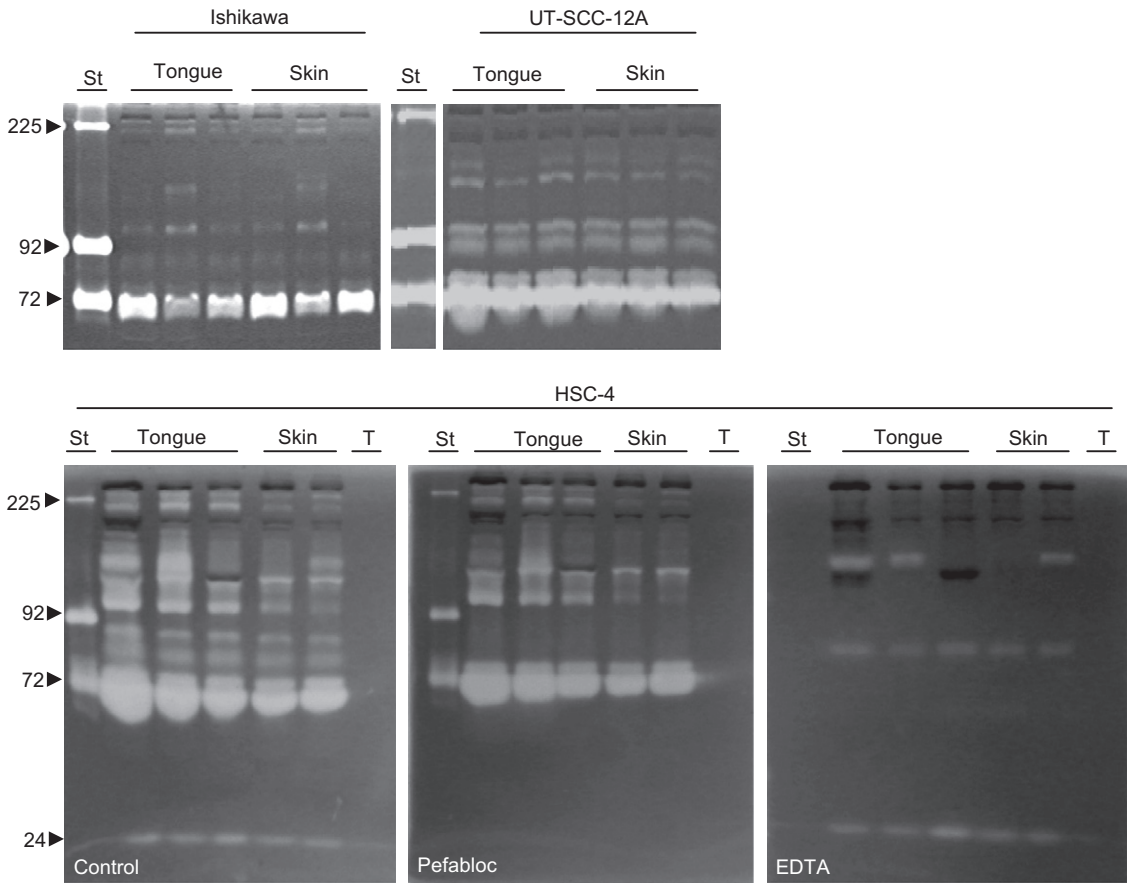

Fig. 7 – Gelatin zymography of plasma. Zymography gels of plasma from parallel mice with tongue or skin tumours of the endometrial adenocarcinoma cell line Ishikawa and the skin SCC cell line UT-SCC-12A (upper panel) and the oral SCC cell line HSC-4 (lower panel). Lower panel: the gels were washed and incubated, as indicated, without (control) or with the following inhibitors: Pefabloc (1 mM) and EDTA (10 mM). The molecular weight standard (St) contains pro-MMP-9 dimer (225 kDa), pro-MMP-9 monomer (92 kDa) and pro-MMP-2 (72 kDa). The lane denoted T contains purified trypsin (24 kDa). Representative gels from at least three independent experiments are shown.

thought to concentrate proteolytic activity at the leading edge of migrating cells.[32] It is likely that the increased gelatinolytic activity in the tumour–stroma interface of the tongue tumours in the present study are due to complex interactions between different proteases produced both by the tumour cells and stromal cells like inflammatory cells and fibroblasts. It is known that fibroblasts from different anatomical sites differ in their transcriptional patterns and can be considered as distinct differentiated cell types.[33] Site specific properties of the fibroblasts and different structural factors such as composition of the ECM and resident immunity may contribute to the differences in gelatinolytic activity and growth pattern of the tongue and skin tumours in this study.

In our tumour model we could see a marked change in morphological features of the cancer cells towards the invasive front of the tongue tumours, with infiltrating cancer cells organised in small groups that had lost their E-cadherin expression. These changes show an EMT-like behaviour of the cancer cells. The EMT-inducing growth factors, transforming growth factor beta (TGF-β) and basic fibroblast growth factor (bFGF) can be released and activated by proteolytic enzymes such as plasmin and MMPs. Further, several MMPs, such as MMP-7, can process E-cadherin.[7–9,34] The observed EMT-like phenotype of the cancer cells at the invasive front of the tongue tumours may therefore be induced by proteolytic enzymes in the tumour–stroma interface such as MMP-7 produced by the cancer cells and MMP-9 produced by neutrophils in the stroma.

Gelatinolytic activity in blood or urine has been shown to correlate with tumour growth and invasiveness, and has been proposed as a prognostic factor in various cancers.[14] Although all cell lines formed more invasive tumours with higher gelatinolytic activity in tongue than in skin, only plasma from mice with tumours of the HSC-4 cell line showed a consistent difference in expression of some gelatinolytic enzymes between mice with tongue tumour and mice with skin tumours. Thus, our results show that the gelatinolytic profile in plasma does not reliably reflect the invasiveness and gelatinolytic activity of the tumours in our model.

Our xenograft model shows that when the same cancer cells are used to establish tumours in tongue and skin, the cells show a remarkably different pattern of growth and

invasiveness, confirming the importance of the microenvironment for tumour progression.

Conflict of interest statement

The work giving rise to the manuscript entitled 'Organ Specific Regulation of Tumour Invasiveness and Gelatinolytic Activity at the Invasive Front' was supported by grants from The Norwegian Cancer Society, The North Norwegian Regional Health Authorities and The Erna and Olav Aakre Foundation for Cancer Research. The study sponsors had no involvement in study design, collection, analyses or interpretation of data or in writing of the manuscript and the decision to submit the manuscript for publication. None of the authors have any relationships with other people or organisations that could inappropriately influence our work. We therefore declare that there is no conflict of interest associated with the submitted manuscript.

Acknowledgments

This work was supported by grants from The Norwegian Cancer Society, The North Norwegian Regional Health Authorities and The Erna and Olav Aakre Foundation for Cancer Research. The authors are indebted to Professor R. Grénman, University of Turku, Finland, and Professor M. Yanagishita, Tokyo Medical and Dental University, Japan for kindly providing the UT-SCC12A and HSC-4 cell lines, respectively. The authors thank Dr. P. McCourt for critical reading and linguistic revision of the manuscript.

REFERENCES

1. Funk GF, Karnell LH, Robinson RA, et al. Presentation, treatment, and outcome of oral cavity cancer: a National Cancer Data Base report. *Head Neck* 2002;**24**:165–80.
2. McGuire JF, Ge NN, Dyson S. Nonmelanoma skin cancer of the head and neck I: histopathology and clinical behavior. *Am J Otolaryngol* 2009;**30**:121–33.
3. Pupa SM, Menard S, Forti S, Tagliabue E. New insights into the role of extracellular matrix during tumor onset and progression. *J Cell Physiol* 2002;**192**:259–67.
4. Kalluri R, Zeisberg M. Fibroblasts in cancer. *Nat Rev Cancer* 2006;**6**:392–401.
5. Fingleton B. Matrix metalloproteinases: roles in cancer and metastasis. *Front Biosci* 2006;**11**:479–91.
6. Folgueras AR, Pendas AM, Sanchez LM, Lopez-Otin C. Matrix metalloproteinases in cancer: from new functions to improved inhibition strategies. *Int J Dev Biol* 2004;**48**:411–24.
7. Yu Q, Stamenkovic I. Cell surface-localized matrix metalloproteinase-9 proteolytically activates TGF-beta and promotes tumor invasion and angiogenesis. *Genes Dev* 2000;**14**:163–76.
8. Cauwe B, Van den Steen PE, Opdenakker G. The biochemical, biological, and pathological kaleidoscope of cell surface substrates processed by matrix metalloproteinases. *Crit Rev Biochem Mol Biol* 2007;**42**:113–85.
9. Noe V, Fingleton B, Jacobs K, et al. Release of an invasion promoter E-cadherin fragment by matrilysin and stromelysin-1. *J Cell Sci* 2001;**114**:111–8.
10. Margulis A, Zhang W, lt-Holland A, et al. Loss of intercellular adhesion activates a transition from low- to high-grade human squamous cell carcinoma. *Int J Cancer* 2006;**118**:821–31.
11. Stahtea XN, Roussidis AE, Kanakis I, et al. Imatinib inhibits colorectal cancer cell growth and suppresses stromal-induced growth stimulation, MT1-MMP expression and pro-MMP2 activation. *Int J Cancer* 2007;**121**:2808–14.
12. Belotti D, Calcagno C, Garofalo A, et al. Vascular endothelial growth factor stimulates organ-specific host matrix metalloproteinase-9 expression and ovarian cancer invasion. *Mol Cancer Res* 2008;**6**:525–34.
13. Elenjord R, Allen JB, Johansen HT, et al. Collagen I regulates matrix metalloproteinase-2 activation in osteosarcoma cells independent of S100A4. *FEBS J* 2009;**276**:5275–86.
14. Vihinen P, Kahari VM. Matrix metalloproteinases in cancer: prognostic markers and therapeutic targets. *Int J Cancer* 2002;**99**:157–66.
15. Yan SJ, Blomme EA. In situ zymography: a molecular pathology technique to localize endogenous protease activity in tissue sections. *Vet Pathol* 2003;**40**:227–36.
16. Hadler-Olsen E, Kanapathippillai P, Berg E, et al. Gelatin in situ zymography on fixed, paraffin-embedded tissue: zinc and ethanol fixation preserve enzyme activity. *J Histochem Cytochem* 2010;**58**:29–39.
17. Grenman R, Pekkola-Heino K, Joensuu H, et al. UT-MUC-1, a new mucoepidermoid carcinoma cell line, and its radiosensitivity. *Arch Otolaryngol Head Neck Surg* 1992;**118**:542–7.
18. Kobel M, Weichert W, Cruwell K, et al. Epithelial hyaluronic acid and CD44v6 are mutually involved in invasion of colorectal adenocarcinomas and linked to patient prognosis. *Virchows Arch* 2004;**445**:456–64.
19. Livak KJ, Schmittgen TD. Analysis of relative gene expression data using real-time quantitative PCR and the 2(-Delta Delta C(T)) method. *Methods* 2001;**25**:402–8.
20. Bjorklund M, Koivunen E. Gelatinase-mediated migration and invasion of cancer cells. *Biochim Biophys Acta* 2005;**1755**:37–69.
21. Clark IM, Swingler TE, Sampieri CL, Edwards DR. The regulation of matrix metalloproteinases and their inhibitors. *Int J Biochem Cell Biol* 2008;**40**:1362–78.
22. Malla N, Sjoli S, Winberg JO, Hadler-Olsen E, Uhlin-Hansen L. Biological and pathobiological functions of gelatinase dimers and complexes. *Connect Tissue Res* 2008;**49**:180–4.
23. Vosseler S, Lederle W, Airola K, et al. Distinct progression-associated expression of tumor and stromal MMPs in HaCaT skin SCCs correlates with onset of invasion. *Int J Cancer* 2009;**125**:2296–306.
24. Schnaeker EM, Ossig R, Ludwig T, et al. Microtubule-dependent matrix metalloproteinase-2/matrix metalloproteinase-9 exocytosis: prerequisite in human melanoma cell invasion. *Cancer Res* 2004;**64**:8924–31.
25. Vilen ST, Nyberg P, Hukkanen M, et al. Intracellular co-localization of trypsin-2 and matrix metalloprotease-9: possible proteolytic cascade of trypsin-2, MMP-9 and enterokinase in carcinoma. *Exp Cell Res* 2008;**314**:914–26.
26. Taraboletti G, D'Ascenzo S, Borsotti P, et al. Shedding of the matrix metalloproteinases MMP-2, MMP-9, and MT1-MMP as membrane vesicle-associated components by endothelial cells. *Am J Pathol* 2002;**160**:673–80.
27. Conese M, Blasi F. Urokinase/urokinase receptor system: internalization/degradation of urokinase–serpin complexes: mechanism and regulation. *Biol Chem Hoppe Seyler* 1995;**376**:143–55.

28. Strongin AY. Mislocalization and unconventional functions of cellular MMPs in cancer. *Cancer Metastasis Rev* 2006;**25**:87–98.
29. Overall CM, Dean RA. Degradomics: systems biology of the protease web. Pleiotropic roles of MMPs in cancer. *Cancer Metastasis Rev* 2006;**25**:69–75.
30. Dano K, Romer J, Nielsen BS, et al. Cancer invasion and tissue remodeling – cooperation of protease systems and cell types. *APMIS* 1999;**107**:120–7.
31. Lund LR, Romer J, Bugge TH, et al. Functional overlap between two classes of matrix-degrading proteases in wound healing. *EMBO J* 1999;**18**:4645–56.
32. Blasi F, Carmeliet P. UPAR: a versatile signalling orchestrator. *Nat Rev Mol Cell Biol* 2002;**3**:932–43.
33. Chang HY, Chi JT, Dudoit S, et al. Diversity, topographic differentiation, and positional memory in human fibroblasts. *Proc Natl Acad Sci USA* 2002;**99**:12877–82.
34. Moustakas A, Heldin CH. Signaling networks guiding epithelial-mesenchymal transitions during embryogenesis and cancer progression. *Cancer Sci* 2007;**98**:1512–20.